











$$MQE_m = \frac{1}{n_U} \sum_{i \in U} mqe_i, \quad n_U = |U| \quad (7)$$

where,

$U$  : the subset of map units.

Hierarchical growth:

Step 1: Check each neuron to find out if its  $mqe_u$  is greater than  $(\tau_2 \cdot mqe_0)$ .  $\tau_2$  is a threshold specifying the desired quality of input data representation at the end of learning process;  $mqe_0$  is the mean quantization error of the single neuron of Layer 0. Then, assign a new SOM at a subsequent layer of the hierarchy.  $mqe_0$  is computed as follows:

$$mqe_0 = \frac{1}{n_I} \sum_{x_j \in I} \|X_{kt} - m_0\|, \quad n_I = |I| \quad (8)$$

where,

$m_0$  : the mean of the input vectors,

$I$  : the set of the input vectors, and

$mqe_0$  : a measurement of the overall dissimilarity of input data.

Step 2: Train the SOM with input vectors mapped to this neuron.

### 3.2.2 Traffic pattern matching

Compute the representative traffic pattern (i.e. cluster seed) of each cluster produced by *GHSOM* by taking the average of all individual traffic patterns being grouping into the cluster. Then the traffic pattern matching algorithm simply assigns the input traffic pattern to a specific cluster with the most similar cluster seed based on the Euclidean distance measure. The process can be summarized as follows:

Step 0: Input a traffic pattern  $X_{kt}$ .

Step 1: Compute the cluster seed of each of clusters.

Step 2: Compute the squared Euclidean distance of each input objects, such that

$$Min(X_{kt}, X_c) = \sum_{i=1}^r (x_k(t+i) - x_c(i))^2 \quad (9)$$

where,

$X_{kt}$  : input traffic pattern and,

$X_c$  : cluster seed of cluster  $c$ .

Step 3: Assign the input pattern to specific cluster with the minimum squared Euclidean distance.

Step 4: Use the prediction patterns of the specific cluster to predict traffic flow.

### 3.2.3 Traffic prediction

The traffic prediction is based on the historical and primitive  $n$  time-series data. Since the

number of traffic patterns needed to construct the prediction model is unknown in advance, GP algorithm is suitable for such prediction. The GP algorithm starts with a population of randomly generated individual trees; each tree corresponds to the linear combination of traffic flow. The traffic prediction contains the following steps:

Step 0: Define function set and terminal set. The function set consists of the arithmetic functions of addition, subtraction, multiplication, division, as well as a conditional branching operator. The terminal set is set as the latest  $r$  periods of traffic flow data.

Step 1: Initialize random population size.

Step 2: Evaluate fitness values of the trees. Randomly select trees from the population, evaluate them with training patterns belonging to this cluster, and then rank them according to their fitness values. A fitness measure is defined as follows:

$$E_{lq} = \sqrt{\frac{\sum_{i=1}^I \sum_{t=1}^h (x_{li}(t+r+1) - f_q(X_{li}(t)))^2}{h}} \quad (10)$$

where

$E$  : fitness measure,

$f_q(\cdot)$  : the mathematical expression of tree  $q$  predicting the traffic flow at next time period based on the inputted historical data at previous time periods, i.e.,  $f_q(X_{li}(1)) = \hat{x}_{liq}(t+r+1)$ .

Step 3: If the fitness value approaches to zero, then stop the procedure. Otherwise, proceed to the next step.

Step 4: Create new individual by applying genetic operations. The genetic operations further include reproduction, crossover and mutation as follows.

Step 4-1: Reproduction. Replace the least-fit two traffic patterns by the best-fit two.

Step 4-2: Crossover. Create a new offspring by randomly combining the chosen parts of two selected trees in each parent tree and swapping the sub-tree rooted at crossover points.

Step 4-3: Mutation. Randomly select a mutation point in a tree and substitute the sub-tree rooted there with a randomly generated sub-tree.

Step 5: Generate new population by using genetic operations, and return to Step 2.

### 3.3 Cell-based Arrival Distribution Modeling

Following Chiou *et al.* (2010), this study employs CTM to predict the arrival distribution of an O-D pair of traffic along a freeway corridor, which is used for computing  $\rho_{ij}^m(k)$ . During free-flow periods, all vehicles in a cell can be reasonably advanced to the next cell as time evolves. One needs not to know where the vehicles are located within the cell. Namely, the system evolution obeys:

$$n_{i+1}(t+1) = n_i(t) \quad \text{for } t = 0, 1, 2, \dots, T \quad (11)$$

where,

$N_i(t) - n_i(t)$  : the amount of empty space in cell  $i$  at time  $t$ .

The traffic flow increases gradually until a queue occurs, where maximum flow and

maximum number of vehicle variables are incorporated into the model.

The CTM assumes a simplified version of the fundamental diagram, typically based on a trapezium form (Figure 3) and provides simple solutions for realistic networks. It assumes a free-flow speed  $v$  at low densities and a backward shockwave speed  $w$  at high densities; both speeds are constant ( $v \geq w$ ).

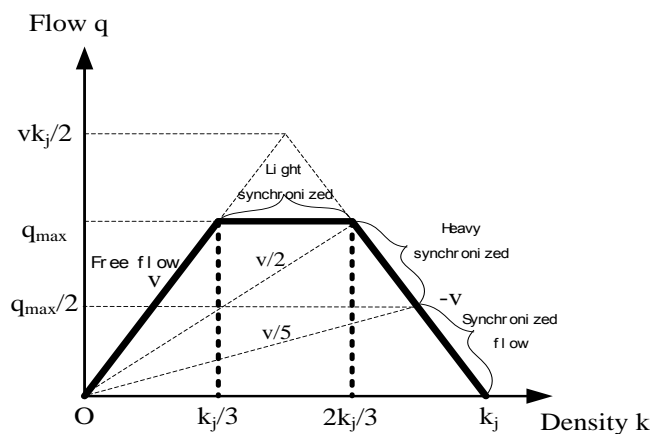


Figure 3. Fundamental diagram of CTM

The number of vehicles flowing into cell  $i$  within time interval  $t$ ,  $c_i(t)$ , is defined as:

$$c_i(t) = \min \left\{ n_{i-1}, \left\lfloor \frac{Q_i}{v} \right\rfloor, N - n_i(t) \right\} \quad (12)$$

If the remained storage capacity and flow capacity in the next cell is sufficient, all vehicles will move forward into the next cell; otherwise, only a portion of them can move into the next cell according to the following logics:

$$\begin{aligned} \text{if } & c_i(t+1) + q_i(t+1) \leq \min [Q_i, N - n_i(t+1)] \\ \text{then } & c_{i+1}(t+1) = c_i(t+1) + r_i(t+1) \end{aligned} \quad (13)$$

$$\begin{aligned} \text{if } & c_i(t+1) + r_i(t+1) > \min [Q_i, N - n_i(t+1)] \\ \text{then } & c_{i+1}(t+1) = 1 - \left[ \frac{\min [Q_i, N - n_i(t+1)]}{c_i(t+1) + r_i(t+1)} \right] \end{aligned} \quad (14)$$

### 3.4 Extended Kalman Filtering

The proposed estimation algorithm, based on the extended Kalman filtering concept, is as follows:

Step 0: Initialization.

Parameters settings include cell length  $L_i$ ,  $i = 0, 1, \dots, N-1$ , and time interval  $t_0$ .

$\text{var}[e(k)] = \text{diag}[r_1, r_2, \dots]$ .  $X(0) = E[b(0)]$ .  $P(0) = \text{Var}[b(0)]$ . Besides, on-ramp, link and off-ramp flows are given.

Step 1: Determine  $\rho_{ij}^m(k)$  by CTM.



Step 2: Compute the linearized transformation matrix based on the determinant  $\rho_{ij}^m(k)$ .

$$H^{K-1} = \begin{bmatrix} H_{rs}^{k-1} \end{bmatrix}$$

$$H_{j, Ni+j-i(i+1)}^k = \sum_{m=0}^M q_i(k-m) \cdot \rho_{ij}^m(k) \quad \text{for } 0 \leq i < j \leq N \quad (15)$$

$$H_{N+1, Ni+j-i(i+1)}^k = \sum_{m=0}^M q_i(k-m) \cdot \rho_{ij}^m(k) \quad \text{for } 0 \leq i < j \leq N \quad (16)$$

$$\begin{bmatrix} H^{K-1} \end{bmatrix} = [h_1, h_2, \dots, h_{2N-1}]^T$$

$$Z'(k) = [y_1(k), y_2(k), \dots, y_N(k); U_1(k) - q_1(k), \dots, U_{N-1}(k) - q_{N-1}(k)]^T$$

Step 3: Initialization of the sequential Kalman filtering method.

Set  $b_0 = b(k+1)$

$p_0 = p_{k+1} + D$ , where  $D = [d_b, \dots, d_b]$  is a covariance matrix of  $W(k)$

Step 4: Sequential Kalman filtering iterations.

For  $i = 1, 2, \dots, 2N-1$

$$g^i = p^{i-1} h_i^T [h_i p^{i-1} h_i^T + r_i]^{-1}$$

$$p^i = p^{i-1} - g^i h_i p^{i-1}$$

$$\delta^i = y_i(k) - h_i b(k-1)$$

Truncation:

$$\alpha' = \underset{0 \leq \alpha \leq 1}{\text{MAX}} \left[ \alpha \left| 0 \leq [b^{i-1}] + \alpha \delta^i g^i \leq 1 \right. \right]$$

$$\text{Set } [b^i] = [b^{i-1}] + \alpha \delta^i g^i$$

Normalization:

For  $m=1, 2, \dots, N-2$

$$\beta_m = \sum_{j=m+1}^N b_{mj}^i$$

$$b_{mj}^i = b_{mj}^i / \beta_m \quad j=m+1, \dots, N.$$

Step 5: Stop condition.

Check the convergence of estimated O-D proportions. If the preset stop condition (convergence level or number of iterations) has not reached, then go to Step 1.

Otherwise, go to Step 6.

Step 6: Prediction of the states.

Set  $p_k = p^{2N-1}$  and  $[b(k)] = [b^{2N-1}]$ ,  $k = k + 1$ , go to Step 1.

## 4. CASE STUDY

The 3-lane mainline freeway stretch of Taiwan Freeway No. 1 between Toufen Interchange and Beidou Interchange is studied due to its dense loop detectors. This stretch is 120 kilometers in length and has 15 on-ramp interchanges in total. An entire week (May 25-31, 2009) of 5-minute traffic counts are directly extracted from the loop detectors throughout this stretch.

### 4.1 Traffic Flow Prediction Models

The entire week of 5-minute traffic counts are separated into a total of 25,935 ( $=1,729 \times 15$ ) traffic patterns with a fixed length of 24 hours on a 5-minute rolling basis. These 25,935 traffic patterns are clustered by GHSOM, which results in a total of 4 layers with 36 different clusters. Note that the number of traffic patterns in each of the 36 clusters ranges from 143 (Cluster 1) to 2,488 (Cluster 6). In each cluster, we then construct a GP traffic flow prediction model based on the traffic patterns in the same cluster. Hence, a total of 36 GP traffic flow prediction models are developed.

Taking Cluster 36 as an example, it contains 488 traffic patterns during the periods of night time to next night time on weekday and weekend in the suburban areas (e.g. Chunghua interchange, Fengyuan interchange, Daya interchange and Nantun interchange) where the maximum 5-minute flow rates can exceed 150 pcu. Figure 4 illustrates four randomly selected traffic patterns, which look similar.

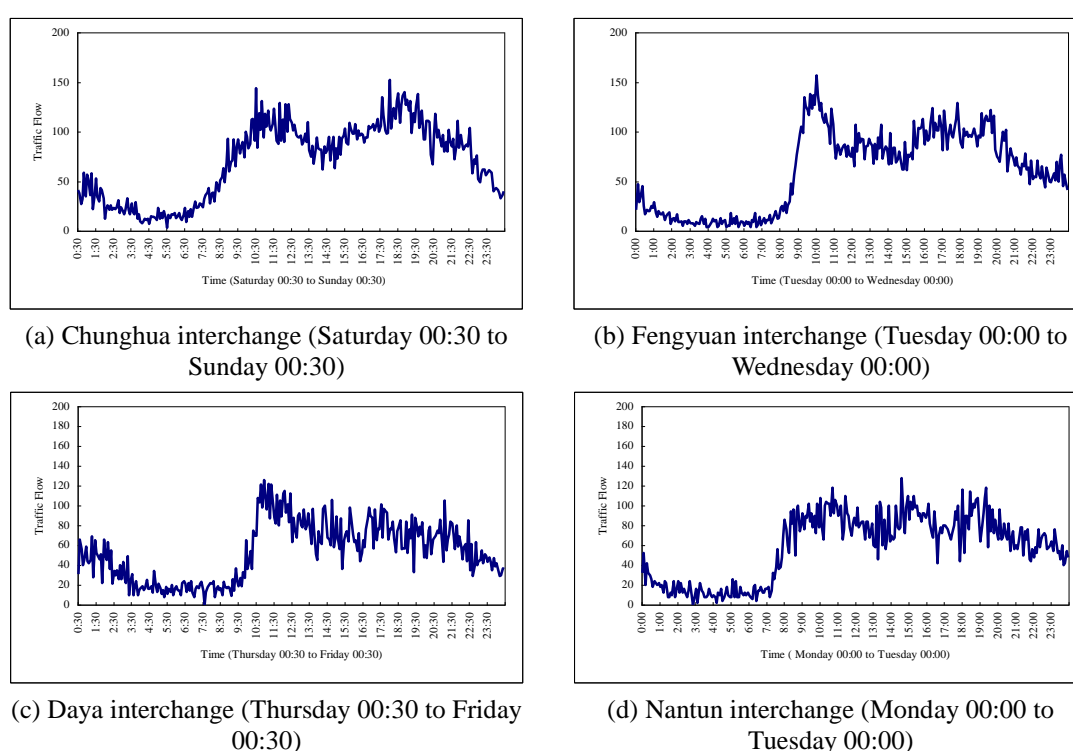


Figure 4. Four randomly selected traffic patterns from Cluster 36 (suburban area)

This study further randomly divides these 488 traffic patterns into two sets: training set (340 patterns) and validation set (148 patterns). Based on the training patterns, the GP traffic prediction model for Cluster 36 is estimated as follows:

$$\begin{aligned}
 x(t+1) = & 0.9967 x(t) + 1.05 \times 10^{-2} x(t-5) + 1.26 \times 10^{-2} x(t-1) x(t-5) - 1.9 \times 10^{-3} x(t-4)^2 - 1.08 \\
 & \times 10^{-2} x(t-3) x(t-5) + 5 \times 10^{-5} x(t) x(t-1) x(t-5) - 4 \times 10^{-5} x(t-1)^2 x(t-4) - 1 \times 10^{-6} x(t-1)^2 x(t-2) \\
 & x(t-5) + 3 \times 10^{-6} x(t-1)^2 x(t-3) x(t-7) - 2 \times 10^{-5} x(t-2) x(t-3) x(t-4) x(t-7) \quad (17)
 \end{aligned}$$

where,

$x(t)$  : the traffic of time  $t$ .

Note from Eq. (17) that the GP prediction model for Cluster 36 only needs the nearest 7 intervals of traffic to predict the very next interval of traffic. With a rolling horizon, the GP

prediction model can repeatedly perform traffic flow prediction for the next 4 hours (a total of 48 time intervals) by feeding-in the newly predicted traffic flow data. The results show that the MAPE values of GP prediction model in training and in validation are 7.02% and 10.75%, respectively, which are satisfactory.

Following the same vein, the GP prediction models for the remaining 35 clusters are developed. Overall, the average MAPE values in training and in validation for the 36 GP prediction models are 6.88% and 10.35%, respectively. It indicates a satisfactory prediction of 4-hour 5-minute traffic flows within this 120-km freeway stretch.

### 4.2 Traffic Arrival Distributions

To show the capability of CTM in replicating the traffic hydrodynamics and to investigate the degree of traffic dispersion under various traffic conditions, simulations on this 3-lane freeway stretch are performed. The parameters are set according to the local situations: free flow speed=100 km/hr, jam density=400 vehicles per kilometer, capacity=6,000 vehicles per hour, cell storage capability=67 vehicles, time interval=6 seconds, and cell length=1/6 km.

Figure 5 shows the arrival distributions under four traffic conditions: free-flow, lightly synchronized flow, heavily synchronized flow, and congested flow. Throughout the simulations, all of the entering traffic flows are increased by the same ratio, step by step, from 10% to 100%. Under free flow condition, it is noted that almost all ranges of arrival times cover only one or two intervals. Under lightly synchronized flow condition, the remaining storage capacity and flow capacity of the next cell are sufficient; hence, all vehicles in a cell can advance into the next cell within each interval. Under heavily synchronized flow condition, the entering traffic has exceeded the remained storage capacity (i.e., flow capacity of the next cell is not sufficient); thus, only a portion of them can move forward proportionally. Under congested flow condition, it is noted that the arrival times of traffic dispersion can be as long as six to eight time intervals.

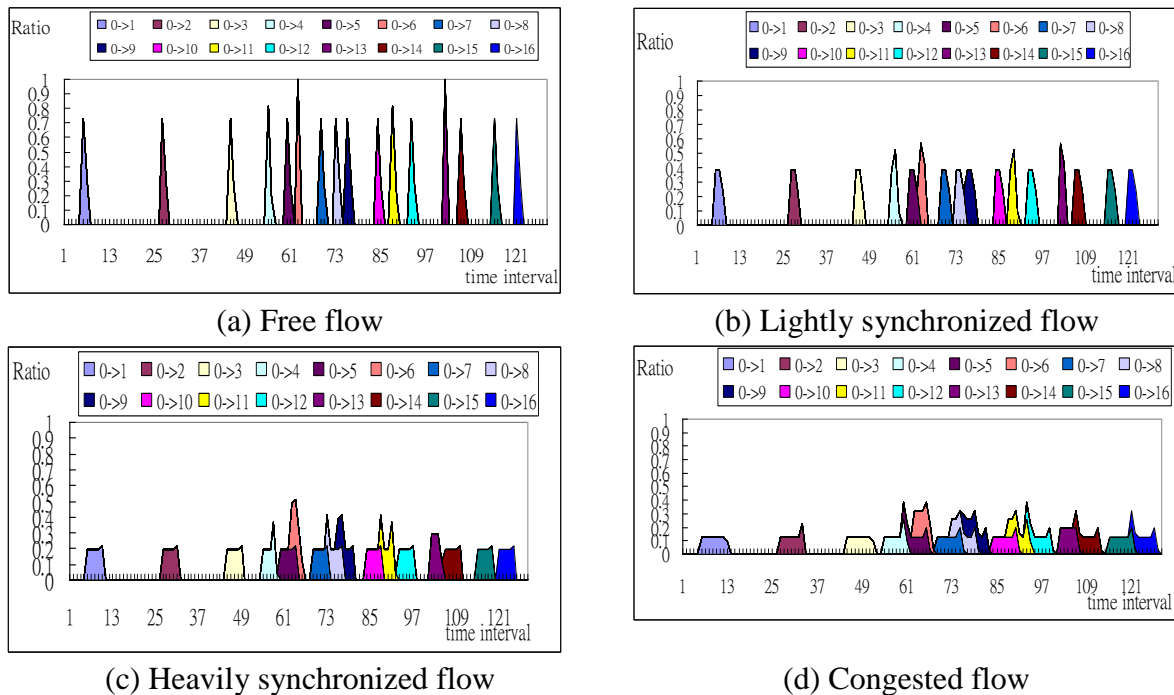


Figure 5. Arrival distributions of entering traffic from origin 0 to various destinations (1~16)

### 4.3 O-D Proportions Estimation

In this study, two initial value settings are attempted: one by randomly generated (RG) technique and the other by equal share (ES) technique. Taking origin interchange No. 12 as an example, the associated O-D proportions are denoted as  $b_{12,13}(k)$ ,  $b_{12,14}(k)$ , and  $b_{12,15}(k)$ . With RG technique, three random numbers 0.2, 0.9, and 0.5 are generated and then normalized such that the sum of three proportions equals 1; namely,  $b_{12,13}(k)=0.125$ ,  $b_{12,14}(k)=0.563$ , and  $b_{12,15}(k)=0.312$ . In contrast, with ES technique, the three proportions are simply set as  $b_{12,13}(k)=0.333$ ,  $b_{12,14}(k)=0.333$ , and  $b_{12,15}(k)=0.333$ .

The distributions of real  $b_{12,15}$  proportions (from Zhanghua Interchange to Yuanlin Interchange) along with the estimated O-D proportions by both RG and ES techniques are demonstrated in Figure 6. Note that the proposed approach can predict real O-D proportions quite accurately for these two initial value setting techniques. However, RG technique seems slightly superior to the ES technique in terms of the prediction accuracy. Thus, the RG technique is adopted for predicting the remained O-D proportions.

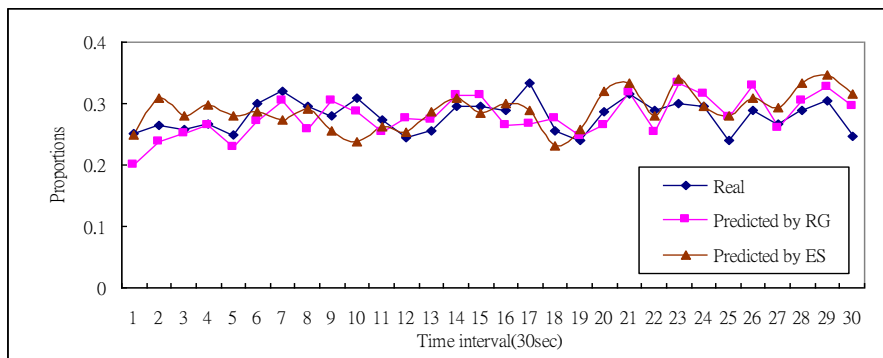


Figure 6. Comparison of real  $b_{12,15}$  proportions with predicted values by RG and ES techniques

Figure 7 illustrates the convergence process for time interval  $k=986$ ,  $b_{1,15}$ , Toufen Interchange to Beidou Interchange. The results show that the overall *RMSE* is 0.1043, indicating a rather high goodness-of-fit of the proposed approach.

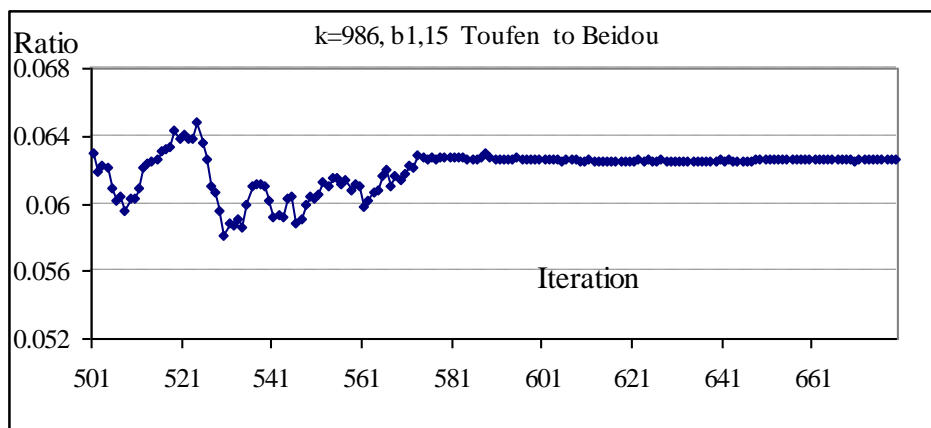


Figure 7. The convergence process

### 4.4 Sensitivity Analysis

Our proposed method heavily depends on the real-time fed-in traffic flow data, which are used for determining which clusters it belongs to, and furthermore, for predicting the traffic flows at the next 48 time intervals. In the previous settings, the traffic patterns have been defined as traffic flow data at consecutive 240 time intervals, or 20 hours. In the following, a sensitivity analysis with different traffic pattern lengths: 48 (4 hours), 72 (6 hours), 96 (8 hours), 120 (10 hours), 144 (12 hours), 192 (18 hours) and 240 (20 hours) time intervals is further conducted. The MAPE values for training and validation are presented in Table 1. We note that shorter lengths (*e.g.*,  $L=48$  and 72) have relatively lower prediction accuracy than longer ones, suggesting the necessity to input a sufficient long traffic pattern for both pattern recognition and prediction. It is also interesting to note that there are no significant changes in prediction accuracy once the length of traffic patterns is longer than 120 time intervals.

Table 1 The MAPE values with different traffic pattern lengths

Lengths	Training	Validation
48	7.29%	19.72%
72	7.78%	14.74%
96	5.32%	12.01%
120	5.72%	10.34%
144	5.91%	10.86%
192	5.63%	10.38%
240	4.58%	10.07%

#### 4.5 Comparison

To show the superior performance of the proposed method, a commonly-used traffic prediction model—the autoregressive integrated moving average (ARIMA) model is further developed for comparison. Following the same data basis as the proposed method, the ARIMA model is also developed on the previous 240 time intervals and predicts the following 48 time intervals. The *MAPE* values of training and validation datasets are 21.77% and 28.65%, respectively, which are much higher than those of our proposed method, which are 5.10% and 10.15%, respectively.

With the self-structured traffic patterns, a simplified prediction model was to be naively developed by averaging the traffic flow data at the last 48 time intervals. For example, if one traffic pattern is of interest in Cluster 1 where 143 traffic patterns have been identified, then the traffic flows at the next 48 time intervals are predicted by taking the average traffic flow of 143 traffic patterns. The *MAPE* values of training and validation datasets for all clusters with this simplified model are 25.21% and 32.73%, respectively, which are much higher than those of our proposed method (4.58% and 10.07%). Again, this comparison further confirms the superiority of the proposed method and it suggests the necessity of GP model.

#### 5. CONCLUDING REMARKS

This paper contributed to propose a novel approach for estimating the freeway dynamic O-D matrices, based on a growing hierarchical self-organizing map and genetic programming, in conjunction with an integrated cell transmission model and extended Kalman filtering to

iteratively estimate the arrival distributions and the O-D proportions, respectively. The case study on Taiwan's freeway has shown that the proposed approach can accurately predict the traffic and estimate the O-D proportions with rather low *RMSE*, indicating its practical applicability.

Several directions for future study can be identified. First, in the case study the O-D matrices are generated by a traffic simulation software—DynaTaiwan based on the detected traffic flows. With advanced traffic surveillance technologies, it is possible in the future to collect real-time traffic information to further validate the proposed approach. Second, the proposed approach is developed only for a freeway corridor. In the future study, route choice behaviors can be incorporated into the proposed approach to extend the applications to a freeway network. Last but not least, a comparison of the proposed approach can be made with other existent O-D estimation algorithms to demonstrate the superiority of different algorithms.

## ACKNOWLEDGEMENTS

This study was partially sponsored by Taiwan's National Science Council under contract number NSC 96-2628-E-009-171-MY3. Three reviewers' constructive comments and suggestions are highly appreciated.

## REFERENCES

- Bell, M.G.H. (1983) The estimation of an origin-destination matrix from traffic counts. *Transportation Science*, 17, 198-217.
- Bell, M.G.H. (1991) The estimation of origin-destination matrices by constrained generalized least squares. *Transportation Research*, 25 B, 13-22.
- Chang, G.L., Tao, X. (1996) Estimation of dynamic O-Ds for urban networks. Proceedings of Thirteenth International Symposium on Transportation and Traffic Theory, Transportation and Traffic Flow Theory, 13, 1-20.
- Chang, G.L., Tao, X. (1999) An integrated model for estimating time-varying network origin-destination distribution. *Transportation Research*, 33 A, 381-399.
- Chang, G.L., Wu, J. (1994) Recursive estimation of time-varying origin-destination flows traffic counts in freeway corridors. *Transportation Research*, 28 B, pp.141-160.
- Chiou, Y.C., Lan, L.W., Tseng, C.M. (2010) Estimation of dynamic freeway origin-destination matrices with cell-based arrival distribution modeling. *Journal of Eastern Asia Society for Transportation Studies*, 7, 1-16.
- Chiou, Y.C., Lan, L.W., Tseng, C.M., Fan, C.C. (2012) Optimal locations of license plate recognition to enhance the origin-destination matrix estimation. *Asian Transport Studies*, 2, 80-92.
- Chiou, Y.C., Lan, L.W., Tseng, C.M. (2013) A novel method to predict traffic features based on rolling self-structured traffic patterns. *Journal of Intelligent Transportation Systems*. (in press)
- Daganzo, C.F. (1994) The cell transmission model: a dynamic representation of highway traffic consistent with the hydrodynamic theory. *Transportation Research*, 28 B, 269-287.
- Hazelton, M. (2001) Inference for origin-destination matrices: estimation, prediction and reconstruction. *Transportation Research*, 35B, 667-676.

- Lin, P.W., Chang, G.L. (2005) A robust model for estimating freeway dynamic origin-destination matrix. *Transportation Research Record*, 1923, 110-118.
- Lin, P.W., Chang, G.L. (2007) A generalized model and solution algorithm for estimating dynamic freeway origin-destination matrix. *Transportation Research*, 41B, 554-572.
- Lo, H., Zhang, N., Lam, W. (1996) Estimation of an origin-destination matrix with random link choice proportions: A statistical approach. *Transportation Research*, 30B, 309-324.
- Rauber, A., Merkl, D., Dittenbach, M. (2002) The growing hierarchical self-organizing map: Exploratory analysis of high-dimensional data. *IEEE Transactions on Neural Networks*, 13(6), 1331-1341.
- Yang, H., Sasaki, T., Iida, Y., Akiyama, T. (1992) Estimation of origin-destination matrices from link traffic counts on congested networks. *Transportation Research*, 26B, 417-434.
- Yang, H. (1995) Heuristic algorithms for the bilevel origin-destination matrix estimation problem. *Transportation Research*, 29B, 231-242.